To the Graduate Council:

I am submitting herewith a thesis written by Peter Ford LaRue entitled "An Evaluation of the Strength of a $SiC_{(p)}/Al_2O_3$ Ceramic Matrix Composite Exposed to Coal Slag at Elevated Temperatures." I have examined the final copy of this thesis for form and content and recommend that it be accepted in partial fulfillment of the requirements for the degree of Master of Science, with a major in Mechanical Engineering.

Dr. R.J. Schulz, Major Professor

We have read this thesis
and recommend its acceptance:

Accepted for the Council:

Associate Vice Chancellor

and Dean of The Graduate School

STATEMENT OF PERMISSION TO USE

In presenting this thesis in partial fulfillment of the requirements for a Master's degree at The University of Tennessee, Knoxville, I agree that the Library shall make it available to borrowers under rules of the Library. Brief quotations from this thesis are allowable without special permission, provided that accurate acknowledgement of the source is made.

Permission for extensive quotation from or reproduction of this thesis may be granted by my major professor, or in his absence, by the Head of Interlibrary Services when, in the opinion of either, the proposed use of the material is for scholarly purposes. Any copying or use of the material in this thesis for financial gain shall not be allowed without my written permission.

Signature Peter L Rn

Date 4-27-95

An Evaluation of the Strength of a $SiC_{(p)}/Al_2O_3$ Ceramic Matrix Composite Exposed to Coal Slag at Elevated Temperatures

A Thesis

Presented for the

Master of Science

Degree

The University of Tennessee, Knoxville

Peter Ford LaRue

May 1995

Abstract

Tubular samples of a silicon carbide particulate reinforced alumina ceramic matrix composite were exposed to Illinois #6 coal slag at temperatures of 1100°C, 1260°C, and 1400°C for a period of 200 hours. Additional samples were held at these same temperatures without the application of slag. Following these exposures, the tubes were cut into C-shaped rings for strength testing. The strength testing was performed by compressing the C-rings at the exposure temperatures using an electric resistance furnace fitted to a hydraulic press. Using a finite element solver coupled to a statistical analysis code, the characteristic strength and Weibull parameter of the material exposed to each of the conditions, was determined. These parameters are used to estimate the probability of failure of a given specimen when subjected to a given set of physical loads.

The strength of the material was found to decrease as the temperature of exposure was increased, with additional decreases caused by exposure to the coal slag. Furthermore, at 1400°C the highest of the three temperatures, a noticeable amount of the tube material was lost. Based on these data, this material's maximum usable temperature range in a high-temperature slagging environment is predicted to lie between 1260°C and 1400°C.

Table of Contents

CHAPTER PAGE

1 Introduction and Background 1

1.1 Introduction 1

1.2 Initial Materials Screening 2

1.3 Changes in Material Properties 3

1.4 Current Research 4

2 Experimental Procedure 8

2.1 Materials Tested 8

2.2 Slag Properties 10

2.3 Exposure Apparatus 11

2.4 Preparation of Mechanical Test Specimens 17

2.5 Mechanical Testing Procedure 23

3 Weibull Analysis of Failure Probability 27

3.1 Background 27

3.2 Equivalent Load Method 29

3.3 Maximum Likelihood Criteria 31

3.4 Summary of Solution Sequence 33

3.5 Restrictions to the Equivalent Load Method 34

3.6 Application of the Equivalent Load Method 35

3.7 Limitations to the Equivalent Load Method 38

4 Results 39

4.1 Strength Data 39

4.2 Trends and Irregularities in the Analyzed Data 42

4.3 Rate of Strength Reduction 47
4.4 Modulus of Elasticity for Tube Sample Materials 48
5 Conclusions and Recommendations 50
List of References 52
Appendices 54
Appendix A. Derivation of Weibull Equations 55
Appendix B. Finite Element Models 58
Appendix C. Statistical Analysis Code 60
Vita 68

List of Figures

FIGURE PAGE

2.1 Optical Micrograph Showing Typical Microstructure of $SiC_{(p)}/Al_2O_3$ Composite 9

2.2 Schematic of Typical C-ring Geometry 12

2.3 Schematic of Slag Dispersal System for Exposure Testing 15

2.4 Photograph of a Tube Exposed to Coal Slag at 1100°C 18

2.5 Photograph of a Tube Exposed to Coal Slag at 1260°C 19

2.6 Photograph of a Tube Exposed to Coal Slag at 1400°C 21

2.7 Finite Element Calculation of the Maximum Principal Normal Stresses in a C-shaped Ring under Compression 22

2.8 Material Testing Unit with a High Temperature (1600°) Furnace Used for Compression Testing 25

4.1 Complete Strength Data 40

4.2 Strength Data for the Tube Material Exposed to Slag at 1260°C as a Function of the Ratio of Modulus of Elasticity of the Tube and Slag Material 46

Chapter 1

Introduction and Background

1.1 Introduction

To economically meet our country's growing power demands while attempting to reduce the environmental effects of producing this power, it is necessary to consider innovative means of power generation. This effort is complicated by projections of reduced availability and increased price of clean, high quality fuels such as sweet crude oil and natural gas. Therefore, the United States Department of Energy (DOE) is encouraging development of a clean efficient means of power generation capable of burning a variety of domestic coals [1].

One component of such a power system will be a high temperature high pressure air heater. Such a heat exchanger would be required to heat a high pressure flow of clean air by extracting heat from a stream of coal combustion products. This environment is recognized as a highly corrosive, and possibly erosive environment which severely limits the choice of construction materials. To achieve the desired levels of efficiency, it is necessary to work with temperatures which, at least in this highly corrosive stream, are above the useful limit for current metallic superalloy materials. Therefore, high temperature structural ceramic materials must be considered for at least the final stage of such a heat exchanger [2].

Unlike the alloy materials currently used in the construction of steam tubes for existing power generation facilities, the properties of many of the ceramic materials which must be considered are not well known. Specifically, additional information

is needed about the strength of these materials during and after exposure to high temperatures and corrosive environments. One of the candidate materials which has been identified is a silicon carbide particulate reinforced aluminum oxide ceramic matrix composite material ($SiC_{(p)}/Al_2O_3$) produced by DuPont Lanxide Composites Inc. The purpose of this study is to evaluate the strength and reliability of this material at elevated temperatures after exposure to a simulated coal combustion environment.

1.2 Initial Materials Screening

Between November of 1988 and September of 1993, a number of Proof-of-Concept Magnetohydrodynamic (MHD) tests were run in the US DOE Coal Fired Flow Facility (CFFF) at the University of Tennessee Space Institute (UTSI) that provided an excellent opportunity to test the effects of this high temperature, highly corrosive, and highly erosive environment on a wide variety of candidate ceramic materials. These tests involved the use of Illinois #6 and Montana Rosebud coals each with the addition of one weight percent potassium carbonate seed as needed for MHD applications. Estimated sample temperatures during these tests ranged from approximately 1100°C to 1600°C.

Many different ceramic and ceramic matrix composite materials were tested during this program. In addition to high temperature corrosion resistance, the effects of thermal shock were highlighted. Of all of the materials tested, a single material provided encouraging results. That material was the $SiC_{(p)}/Al_2O_3$ ceramic matrix composite produced by Lanxide [3].

This material, which is produced by an innovative process developed by Lanxide known as Directed Metal Oxidation (DIMOX^{TM}), demonstrated a strong resistance to high temperature corrosion along with excellent resistance to thermal

shock. In later tests, no significant loss of material was found to occur after several hundred hours at specimen temperatures up to approximately 1400°C. However, at approximately 1450°C, rapid material removal was experienced in a much shorter period of time. This provided an initial estimate of the useful upper limit of the material as occurring somewhere between 1400°C and 1450°C in this environment [4].

1.3 Changes in Material Properties

The initial screening of a variety of materials in the CFFF indicated that most of the candidate materials were clearly unsuitable for use in this environment due to rapid corrosion or high sensitivity to thermal shock which occurred during facility shutdown or change of test conditions. Therefore, additional study at UTSI was focused on further evaluation of the DIMOX^{TM} composite material from Lanxide. That material showed no serious significant signs of physical degradation after exposure to most of the conditions to which it was exposed. However, no information was obtained about the possible changes in the material mechanical properties from exposure to the high temperature slagging conditions. A preliminary study of the changes in the strength of the material was clearly needed.

In 1992, a study was conducted by Jon Winkler[5] at UTSI involving mechanical testing of circular rings cut from a tube exposed during one of the MHD tests in the DOE CFFF. This study compared the properties of the material, as it was received from the manufacturer, with samples which had been exposed to slag at a tube temperature of approximately 1230°C for 107 hours. The tests showed a very slight decrease in characteristic strength after exposure, along with a decrease in Weibull parameter [5] that characterizes the material failure probability. These

data indicated that, while the typical fracture stresses did not change much, the amount of scatter in the data increased.

While that study provided a much needed first look at the changes in the strength of the material, it was limited in a number of ways. The first limitation was the lack of control of the exposure conditions to which the material was subjected. Since the material was exposed during a field test, the exact conditions of exposure were difficult to accurately describe. The second limitation was that the the strength of the material was tested at room temperature rather than at the exposure temperature. Winkler's testing provided the opportunity to highlight property changes, but did not produce strength values which could be used to predict the likelihood of the material failing when loaded at its working temperature. A third limitation of the study was that only a small number of samples were tested. This makes the results less reliable and more difficult to interpret. Finally, the material tested was exposed to only a single exposure condition, or temperature (1230°C), for a 107 hour duration.

1.4 Current Research

As a result of the Department of Energy's continued interest in evaluation of candidate materials for a high temperature air heater, a number of research programs are currently being supported. Each of these programs is intended to complement the others. In addition to developing a database of material properties expressed as failure statistics, these programs will provide a comparison of the cost and reliability of a variety of methods of evaluating the effects of corrosion on high temperature structural ceramics [1]. To achieve this goal, the experimental setup at each of the material evaluation sites is different. Because the initial screening of materials done at UTSI involved what was considered a "worst case" in terms

of harshness of environment, some materials which were found to be unsuitable during that testing are still being studied in the current phase of research.

The first of these programs involved exposure of coupons of a number of materials to a static bath of coal slag at elevated temperatures by researchers at the University of North Dakota Energy & Environmental Research Center (UNDEERC) [6]. The visible effects of this exposure were studied, and then the samples were sent to Oak Ridge National Labs for strength testing. This extensive test program explored the relationships between a number of parameters. Three different materials were considered: β-SiC from Coors Ceramics Company, NT230 siliconized SiC from Saint-Gobain/Norton, and the $SiC_{(p)}/Al_2O_3$ ceramic matrix composite material from DuPont Lanxide. In addition to testing materials both in the as-received condition and after exposure to slag, a variety of stressing rates were used. That study provided a wide variety of useful information [6].

Of relevance to this study, the material from Lanxide showed a significant loss of strength between room temperature and 600°C and continued to weaken as the fracture temperatures were increased as high as 1400°C. None of the materials showed much variation in strength due to stressing rate, except for the Lanxide material at 1400°C. At this temperature, the material demonstrated excessive creep, and could not be tested to fracture at low stressing rates. On the other hand, the Lanxide material showed the least amount of loss in fast fracture strength due to exposure to coal slag at the test temperatures of 1100°C and 1260°C. The resulting strength was approximately 5% to 15% lower than that of unexposed samples tested at the same temperatures, depending on the test temperature and slag type.

The second program, which is the topic of this report, involves a slight increase in the complexity of the exposure procedure. This program at the University of

Tennessee Space Institute involves exposure of tubular samples of the Lanxide material to a periodically refreshed bath of pulverized Illinois #6 coal slag. Because of the interest in MHD applications at UTSI, this study is limited to evaluation of only the Lanxide material, which has demonstrated an initial resistance to chemical attack under these harsh conditions. By periodically refreshing the coal slag applied to these samples, instead of using a static slag bath as in the tests done at UNDEERC, the test conditions are expected to more closely simulate the true environment of a high temperature air heater.

This work is funded by a joint university/industry research grant from the US DOE entitled, "High Performance Materials in Coal Conversion/Utilization". This three year grant was awarded to UTSI in October of 1993. The University of Pennsylvania and Lanxide Corporation are both subcontractors under UTSI program management. The stated objective of the grant is to "test, analyze, and improve the heat and coal slag resistance of Lanxide's $SiC_{(p)}/Al_2O_3$ DIMOX^{TM} ceramic composite tubular material." In addition to the study of the strength of the material after exposure to coal slag at elevated temperatures, laser application of protective coatings is also being explored at UTSI. Researchers at the University of Pennsylvania are charged with developing a theoretical model of the reactions which occur when the material is exposed to a hot stream of coal combustion products. In addition to supplying the materials needed for the other tasks, Lanxide Corp. has been exploring new ways to produce the materials which will result in reduced cost, improved properties, and better dimensional tolerances.

A third program currently in its early stage consists of testing done at Oak Ridge National Labs at an additional level of complexity. This program will involve periodic addition of coal slag to ring samples of the candidate materials while they are being subjected to a physical load. This will help to determine whether stresses

in the material will have a significant effect on the reduction of the strength of the materials due to exposure to the corrosive coal slag [7].

Chapter 2

Experimental Procedure

2.1 Materials Tested

The materials supplied for this task consisted of ten DIMOX^{TM} tubes, each approximately 183cm (6 feet) long with a 51mm (2 inch) outside diameter and a wall thickness of approximately 4.5mm (0.18 inches). This material came from a production run and represents commercially available material. Lanxide's material designation for this material was 93-X3063. Figure 2.1 shows the typical microstructure for this material. It is reported to consist of 47-48 percent, by volume, SiC particles with diameters from 5 to 20 microns, 40% Al_2O_3, and 12% Al-Si Alloy (> 8% Si) with 1-2% residual porosity.

When these tubes arrived at UTSI they were inspected for obvious flaws or damage, but none was observed. Each of the tubes was assigned a number from one to ten corresponding to its position in the shipping container. The ends of the tubes were then marked to specify orientation within the shipping crate. The primary reason for this labeling was simply to provide a consistent method of referring to and labeling the test samples as they were cut from these tubes. One additional mark was applied to each of the tubes. This consisted of a line extending the length of each tube designating a top surface for the tube. This was later used as the top surface during exposure and as the maximum stress location during mechanical testing. Initial sectioning of these tubes was done using a slightly modified, water cooled Clipper brick saw with a 14 inch diameter, 0.125 inch thick

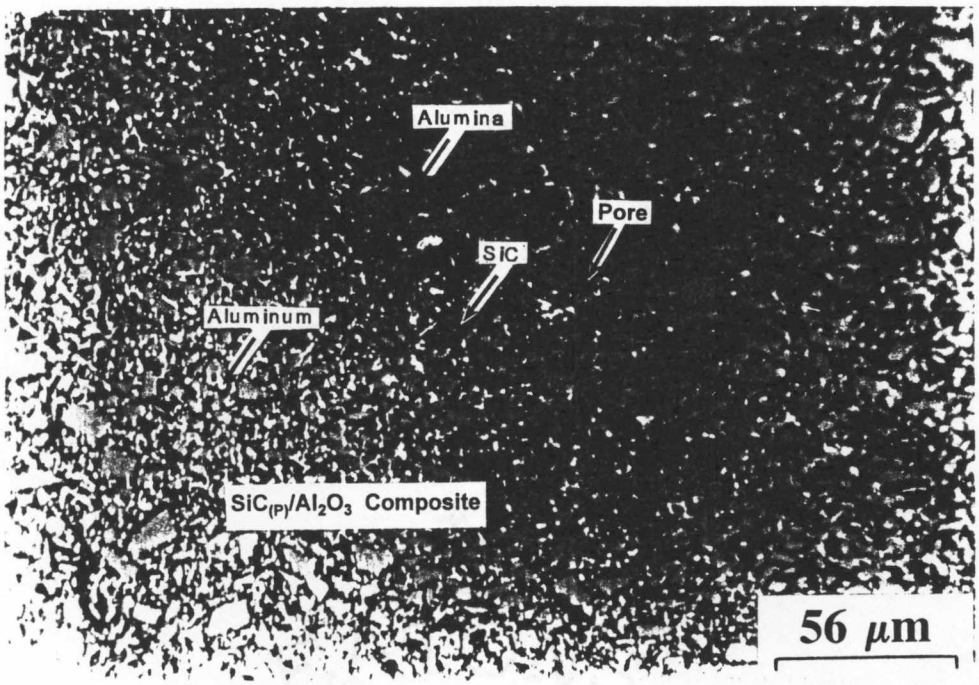


Figure 2.1 Optical Micrograph Showing Typical Microstructure of $SiC_{(P)}/Al_2O_3$ Composite

diamond laced blade. This produced rather rough cuts, but was the only piece of equipment available which could handle a full length tube.

2.2 Slag Properties

The slag used came from a boiler at Southern Illinois Power Cooperative and was produced by the burning of Illinois #6 Coal in air under typical power utility conditions. The chemical composition of the slag was found to be a reasonably good match for typical Illinois #6 slag. A summary of the results of a slag analysis done at UTSI, normalized to yield a total of 100%, is given in Table 2.2.

Table 2.2

Test Slag Composition

Compound	Relative Amount (by mass)
SiO_2	47.76%
Fe_2O_3	19.79%
Al_2O_3	16.57%
CaO	10.37%
MgO	2.62%
K_2O	1.48%
TiO_2	0.85%
Na_2O	0.37%
SO_3	0.19%

When the slag arrived at UTSI, it was made up of granules with an average maximum dimension of 1 to 2 mm. Preliminary testing showed that if this material was dropped onto a tube surface, it would simply bounce off. Therefore, the slag was pulverized to a fine powder using a Braun direct drive pulverizor, until it would

fit through an ASTM standard #60 wire mesh sieve. Thus the slag powder applied to the tube samples during testing consisted of particles no larger than 250 μm.

2.3 Exposure Apparatus

The purpose of the exposure apparatus was to attempt to simulate the environment of a coal-fired exhaust stream. Six different conditions were to be simulated. The first of the parameters needed to describe each of the conditions was the test temperature. Three temperatures were chosen to correspond to the temperatures used by the related research projects discussed in Chapter 1. These temperatures were 1100°C, 1260°C, and 1400°C. The second parameter needed simulate the exposure conditions was the presence or absence of coal slag. A method for applying the coal slag was devised and the coal slag was applied at one hour intervals during the test periods. Each of the exposure tests lasted for a period of 200 hours. For each test condition, two tubes, each approximately 25cm long, were exposed. This produced a sufficient amount of strength-test material to produce 40 mechanical test specimens which were 10mm wide C-shaped rings as shown in Figure 2.2 for each of the conditions. Table 2.1 provides a summary of the exposure conditions used.

Table 2.1

Summary of Exposure Conditions

Temperature	With Slag	No Slag
Room Temp		40 Rings
1100°C	40 Rings	40 Rings
1260°C	40 Rings	40 Rings
1400°C	40 Rings	40 Rings

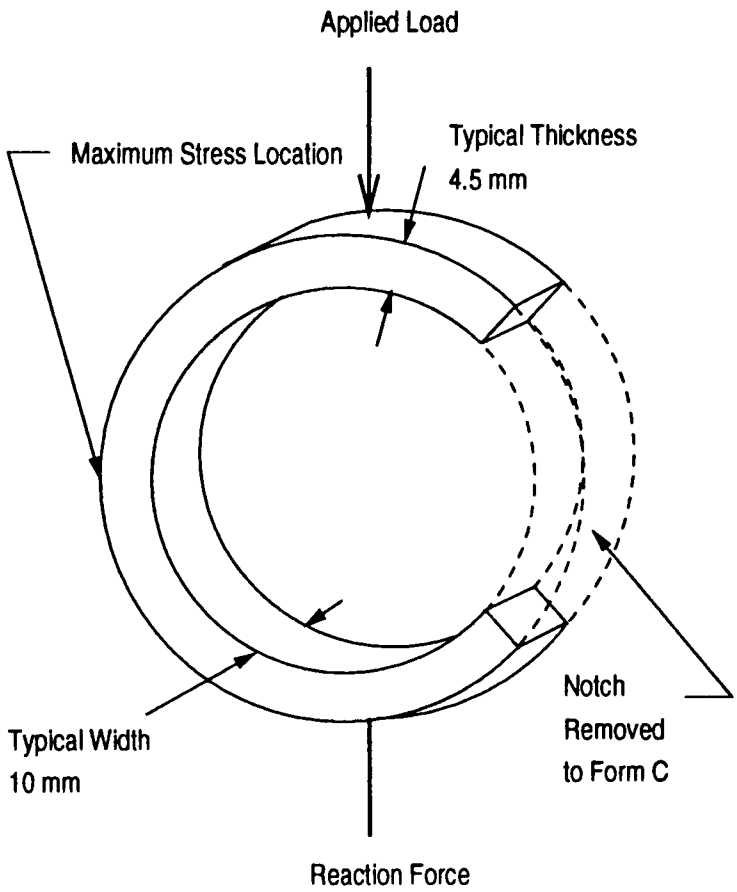


Figure 2.2 Schematic of Typical C-ring Geometry

The exposure temperatures were achieved and maintained inside two Pereco^{TM} electric resistance furnaces. One of these furnaces was modified for use with the exposures requiring the addition of slag, while the other was kept slag free to avoid unintentional sample contamination. For each of the three desired exposure simulation temperatures, two sample tubes were placed on the shelf of the clean furnace oriented according to the marks made on the full length tubes from which they were cut. The furnace temperature was then brought up to the desired level at a rate of approximately 100°C per hour. Once that temperature was reached, it was held constant for a period of 200 hours. At the end of 200 hours, the temperature was allowed to decrease at a rate not greater than 100°C per hour. After the first few hours of the cooling period, the power-off cooling rate fell below this rate. At that point the furnace was simply turned off, and allowed to cool at its natural rate until room temperature was reached. After cooling completely, the furnace was opened, and the sample tubes were removed. The orientation of the sample tubes within the furnace was used as a basis for remarking the top side and end orientations on the tubes. This was necessary because the previous markings were destroyed by the high temperatures.

The experimental setup for exposure testing required for those sample tubes which were to be exposed to coal slag at the elevated temperatures was more complex. Three modifications to one of the furnace environment were made. First, it was deemed desirable to keep a visual record of the exposure process. During the earlier material screening tests in the DOE CFFF, video records of the exposures had been kept. These videos provided qualitative information about the physical properties of the slag layer including an order of magnitude estimate of the amount of slag coming into contact with the tube. It was hoped that a similar record kept of these exposures during these present tests would also provide useful information.

To accommodate this process, a view port was installed in the exposure furnace, and a time compression video system was set up so that a full record of each 200 hour test could be kept on 2 standard VHS video cassettes. Unfortunately, the contrast of the videos produced by this system was not sufficient to allow much information to be gained. Therefore, while a video was made during each of the exposures, analysis of them has not been done.

The second required modification to the exposure system was a slag containment system. Because of the highly corrosive nature of the slag at high temperatures, it was considered important to keep any slag which fell off of the sample tube from directly contacting the furnace walls or floor. To avoid this problem, a bowl was constructed of Greenpak-85-P, an 85 Vol% alumina, phosphate-bonded plastic refractory produced by A.P. Green Industries of Mexico, Missouri. According to their catalog [8], this material is intended to have a high strength and excellent slagging resistance. While this method of containment seems to have worked reasonably well at the lower two temperatures, some seepage of the slag was evident at 1400°C. As a result, at the highest simulation temperatures some damage occurred to the exposure furnace. Several of these bowls were made and used throughout the test program.

The final, and most complex of the additions made to the furnace was incorporation of a slag dispersal system. The slag dispersal system was designed to be an automated system which would apply approximately 1 cubic centimeter of pulverized slag per linear centimeter of tube, once per hour, over a period of 200 hours. The slag delivery rate was chosen based on calculated tube slagging rates in the CFFF based on video tape recordings of the exposure tests performed in the CFFF.

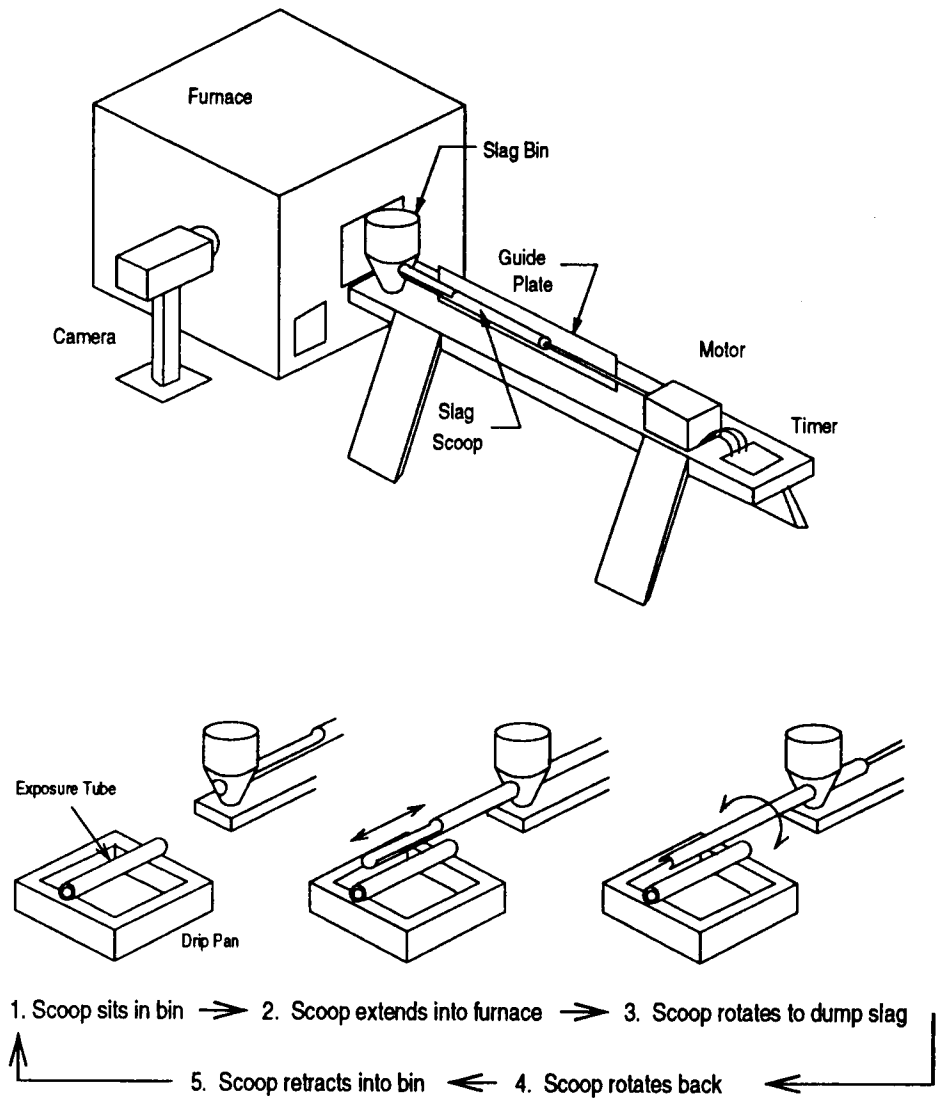


Figure 2.3 Schematic of Slag Dispersal System for Exposure Testing

The powdered slag was placed in a slag bin as seen in Figure 2.3. At one hour intervals, an electric motor would slowly push a slag scoop through the slag bin, where it would fill with slag, and then pass on into the furnace, where it would then be rotated to dump the slag onto the exposure tube. The slag scoop would then quickly be retracted before being damaged by the high temperatures inside the furnace. The slag scoop consisted of a piece of stainless steel pipe cut in half lengthwise to form a semi-cylindrical trough. The scoop drive mechanism consisted of a high torque 12 volt DC motor driving a threaded rod. By rotating the threaded rod in a nut attached to the rear end of the slag scoop, the scoop was pushed forward. A slotted guide plate was used to keep the slag scoop from rotating until it reached its fully extended position, at which point it experienced a 180° revolution thereby dumping the slag from the scoop. The timing of the system was controlled by an analog electric timer.

The procedure used for the slagging exposures was very similar to that used when not applying slag. For each test, a single ten inch long tube sample was positioned inside the furnace such that it would lie directly beneath the slag dispersal system with its top position facing upward. The furnace was closed, and a single run of the slag dispersal system was used to verify the accuracy of the tube positioning. If necessary, the tube position was adjusted. The furnace temperature was then brought up to the desired level at a rate of approximately 100°C per hour. Once the desired temperature was reached, the timer on the slag dispersal system was started, and the video monitoring system was activated. After 200 hours, the slag dispersal system was run a final time, and then the furnace temperature was allowed to decrease at a rate not greater than 100°C per hour. As a result, each tube sample had slag applied 201 times at high temperature, in addition to the test dump at room temperature before turning on the furnace.

Several times during the test program, an exposure test had to be aborted because of electrical power failures, which resulted in premature cooling of the furnace. When this occurred, the furnace was shut down so that it would not reheat when the power returned. Instead, it was allowed to cool completely, and a new test was begun using a fresh tube sample when power was restored.

2.4 Preparation of Mechanical Test Specimens

The exposure testing produced twelve, ten inch long, exposed tubes representing six different exposure conditions. To evaluate the strength of the tube material after exposure to the different test conditions, it was necessary to cut the exposed tube samples into C-shaped rings, each approximately 10mm wide. These samples were cut using a Mark V high speed saw with a thin 15 cm diameter continuous rim diamond laced blade. In two cases, the slag layer on the tubes had to be modified before cutting the tubes into rings. Those tubes which were exposed to slag at 1100°C developed a tall ridge of slag running the length of the tube as seen in Figure 2.4. The friable nature of this slag coat made it easy to remove without damaging the underlying ceramic tube material. Therefore, prior to cutting, the appearance of these tubes was returned to a state very similar to that of those tubes which had been heated without exposure to slag.

Those tubes which were exposed to slag at 1260°C also showed a considerable buildup of slag as seen in Figure 2.5. However, this slag covering was much more irregular, and also much stronger. This slag formed a hard glassy structure full of air bubbles. Because it was strongly bonded to the surface of the ceramic tube material, it was not possible to remove it completely without damaging the base material to be tested. Therefore, it was only partially removed. The brick saw

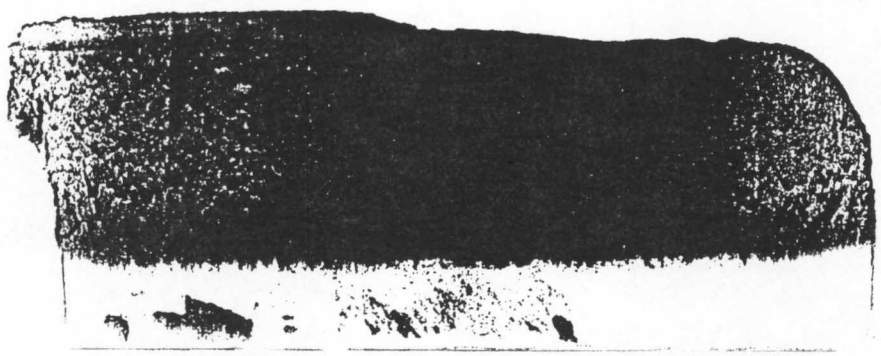


Figure 2.4 Photograph of a Tube Exposed to Coal Slag at 1100°C

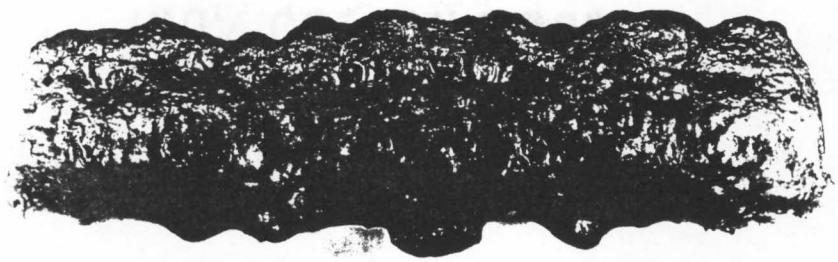


Figure 2.5 Photograph of a Tube Exposed to Coal Slag at 1260°C

described earlier was used to remove large portions of the slag coat. The tube was then cut using the high speed diamond bladed saw to produce the ring samples.

Exposure to slag at 1400°C left a very thin glassy slag coating on the material as seen in Figure 2.6. Due to the thin nature of this slag coating, no preparation of the outer surface was done prior to preparation of rings samples.

Once the preliminary slag removal had been completed, each of the ten inch long tubes were cut in half using the high speed diamond cutoff saw. Then, beginning at the newly cut surface, and working toward each end, a total of 20 circular rings were cut. This left an unused a stub of material from each end of the exposure tube. The unused ends were not tested because any non-uniformities in the slag dispersal process at the ends of the tubes may result in increased scatter in the strength data obtained from testing C-rings cut from the ends.

Once the circular test rings were formed, a notch covering one fourth of the circumference of the ring was removed. This notch was positioned to be centered opposite the portion of the ring which had been facing upward during the exposure testing. The resulting geometry was shown in Figure 2.2. The notch allowed the location of the maximum tensile stresses, by compressive loading of the resulting C-shaped rings, to coincide with the location of maximum slag contact during exposure as described in Figure 2.7.

Initially, it was believed that a full circular ring would provide this property. However, theoretical calculations, which were performed based on the theory of elasticity, showed that such a configuration would have resulted in slightly higher stresses on the inside surface of the tube near the location of load application than would occur at the outside surface where the corrosion effects on strength were to be studied. Furthermore, to produce maximum tensile stresses on the outer surface of a circular ring, it is necessary to load the rings in tension. Due to the



Figure 2.6 Photograph of a Tube Exposed to Coal Slag at 1400°C

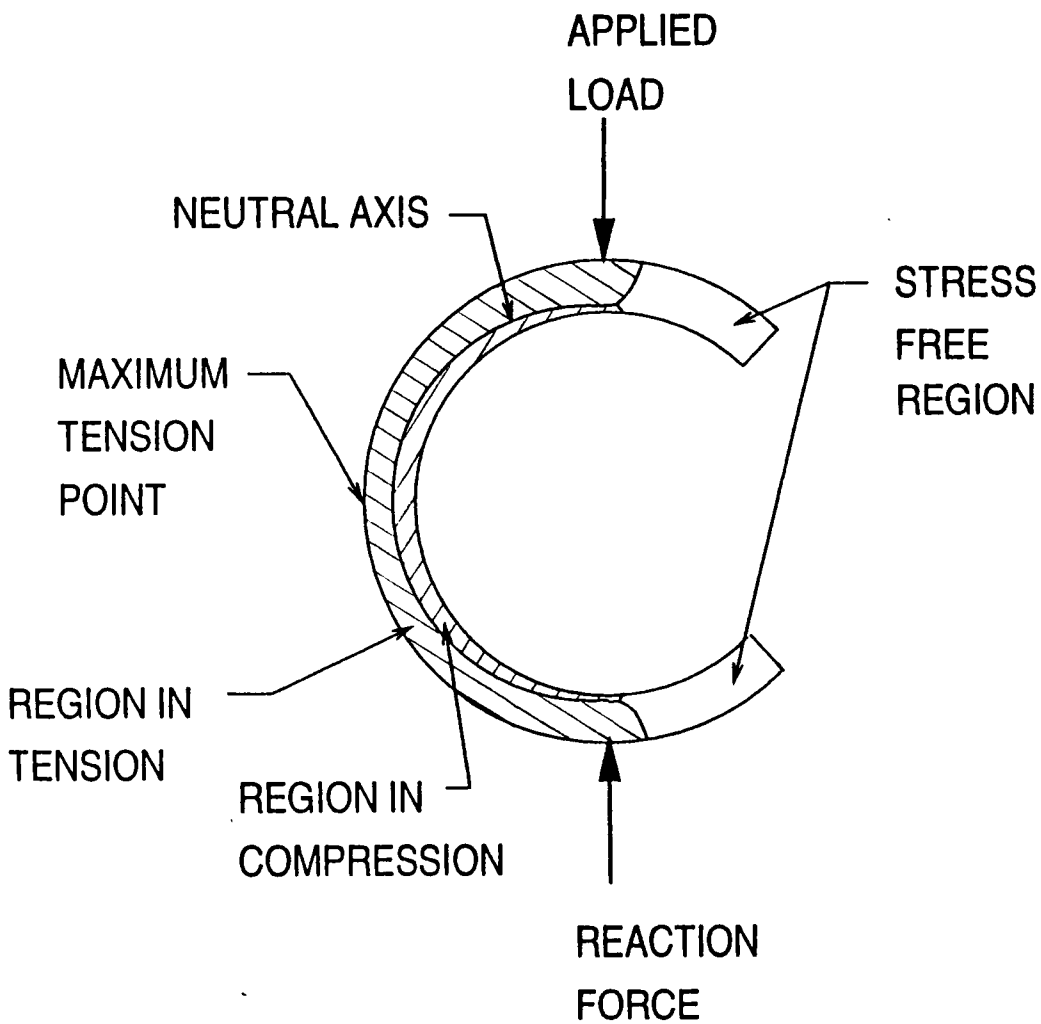


Figure 2.7 Finite Element Calculation of the Maximum Principal Normal Stresses in a C-shaped Ring under Compression

difficulties associated with applying a tensile load at elevated temperatures, the decision was made to test C-shaped rings.

After the C-shaped rings were cut, some surface preparation was needed to reduce the effects of machining damage on the strength of the material. This was done by grinding the cut surfaces with a 60 Grit SiC wet sanding disk. While additional surface preparation may have further increased the measured strength of the samples, the availability of time and equipment imposed this limit.

After surface preparation, a number of measurements were made on each sample in an effort to describe the geometry of the specimen. The measurements taken consisted of a width and a thickness value measured at five locations equally spaced around the portion of the specimen which would be stressed during testing. The geometry of the tubes as-received from Lanxide was such that the outside diameter of the tubes was nearly uniform, while the inside surface was much more irregular. Therefore, the outside diameter was assumed to be constant in the as-received condition. Furthermore, except for the tubes exposed to slag at 1400°C, no measurable changes in the sample geometry was observed. However, for the tubes that were exposed to the most extreme temperature and slagging condition, a noticeable amount of material was destroyed during exposure. Therefore, for those tubes, the outside diameter of the tube was also measured at a number of locations.

2.5 Mechanical Testing Procedure

The mechanical testing was done using a hydraulic universal testing machine built by MTS Corp. of Eden Prairie, Minnesota. A high temperature furnace was added to this system to allow the strength testing to be performed at the same temperature at which the exposure had occurred. The test procedure began with

the mounting of a sample between the two SiC platens of the test machine enclosed by a furnace as shown in Figure 2.8. A small preload compressive force of 20 to 70 Newtons was applied to hold the specimen in place. The furnace was then closed, and power was applied. Following the furnace manufacturer's recommendations, a heating rate not greater than 50°C per minute was used. Throughout the heating process, continuous adjustment of the platen positions was necessary to counteract the thermal expansion of the SiC push rods and maintain a preload between 20 to 70 Newtons If no adjustments had been made, the thermal expansion would have been sufficient to fracture the samples before reaching the desired temperature.

Once the furnace temperature controller indicated that the desired temperature for fracture testing had been reached, a short waiting period of approximately 5 minutes was used to allow thermal equilibrium to be established within the furnace, and for the rate of thermal expansion of the push rods to become negligible. Once this had occurred, the sample was loaded by compressing it at a rate of 0.5 mm per minute. The resulting load-defection curve was recorded using a single channel Linseis strip chart recorder and the maximum load value was recorded by the MTS controller. For each test, the maximum load at fracture was recorded, and the slope of the load deflection curve was obtained for computation of the elastic modulus of the specimen.

After fracture, the furnace was turned off and allowed to cool at its natural rate. This cooling process typically required 30 to 45 minutes before the furnace was cool enough to open and unload. The samples usually broke into two pieces with the fracture occurring near the maximum stress point. However, several samples broke into three pieces, and a few samples produced four pieces. In the cases in which more than one fracture occurred, the primary fracture was easily identified by the location of a compression lip at the inside surface. In contrast,

the secondary fractures usually showed a compression lip on the outside surface indicating a fracture caused by an elastic reaction to the applied bending forces when the forces were relieved by the initial fracture. The resulting broken pieces were then placed in a marked envelope for storage and the process was repeated for the next sample.

One problem which caused a number of delays in testing was the tendency of the furnace heating elements to break. The location of the elements which broke during testing was always opposite the notch cut to produce the C-shaped test rings. This, along with the observation of additional bruising of the heating elements in this area led to the conclusion that the heating elements were damaged by the impact on them of broken specimen pieces produced during testing.

To reduce the damage to the heating elements by impact fragments, a thin covering of ceramic fiber insulation was placed in front of them. Resulting tears in this protective layer provided additional evidence that the damage of the heating elements was at least partially due to impact of pieces of fractured test specimens. While this insulation reduced the amount of damage done to the heating elements, it did not eliminate it completely. To do so would require a significant amount of redesign of the furnace interior.

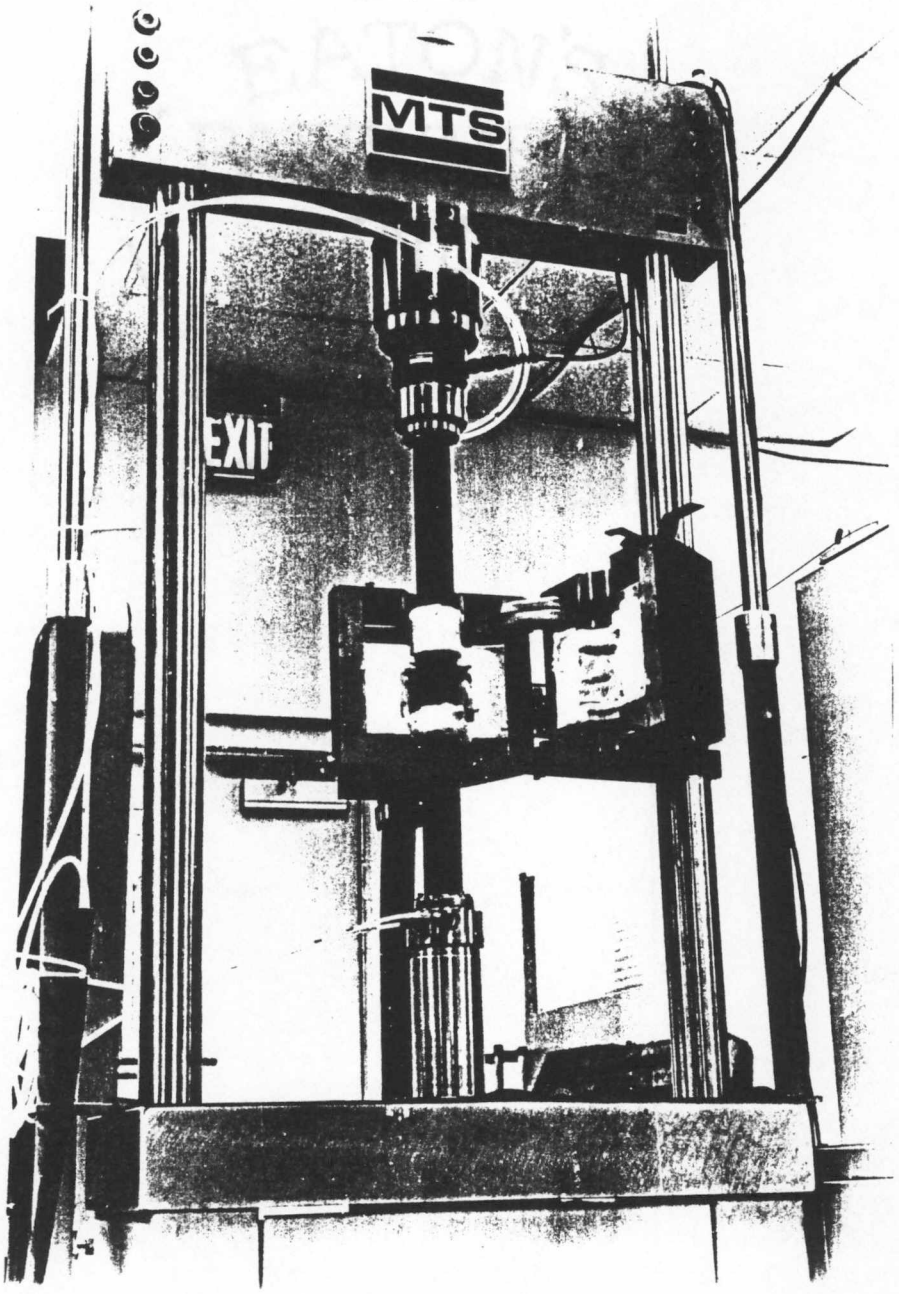


Figure 2.8 Material Testing Unit with a High Temperature (1600°) Furnace Used for Compression Testing

Chapter 3

Weibull Analysis of Failure Probability

3.1 Background

Deterministic design techniques are usually adequate for metallic materials subject to static loads or under low cycle loads. However, statistical techniques are required for failure estimates of ceramics and also metallic materials undergoing highly cyclic stress loadings. For ceramics, the need for a statistical approach to failure estimates is largely due to the brittle nature of ceramics and their sensitivity to flaws. Therefore, while the strength of a metal is typically described by a single yield stress or ultimate tensile stress value, the fracture strength of a ceramic is described by a statistical distribution.

The strength distribution of a ceramic material is usually described by either a two-parameter or a three-parameter Weibull distribution [9,10]. The three parameter distribution is only used when there is no probability of failure at stresses maintained below some specified level. Since this is not normally the case, the two-parameter Weibull distribution is more commonly used [9,10].

The two-parameter Weibull distribution is given by

$$F = 1 - e^{-KA(\frac{\sigma_{max}}{\sigma_o})^m} \tag{1}$$

where F is the probability of failure, σ_{max} is the maximum stress value in a specimen, σ_o is the characteristic strength, and m is the Weibull parameter. In this equation σ_o and m are material properties which are assumed to be independent

of geometry and loading conditions. The characteristic strength σ_o represents the stress level which, if present across a unit surface area of material in uniform tension would result in a 63.2% probability of failure. The Weibull parameter m, which was initially considered as a purely empirical constant useful for describing the amount of variation in probability of failure, has been shown to be related to the flaw size distribution in the material to be Tested [11].

In Equation 1, KA is an effective area term defined as

$$KA = \int \left(\frac{\sigma}{\sigma_{max}}\right)^m dA \tag{2}$$

where σ is the stress distribution in the specimen and dA is a differential element of the surface area of the specimen. It is this term which contains the geometry and load configuration dependent terms. A similar expression for effective volume KV can be substituted for KA throughout this analysis if the critical flaws in the material are volume distributed rather than located at the surface as is the case in this study. The stress terms such as σ, σ_o, and σ_{max}, are all maximum principal normal stresses. The maximum principal normal stress is the largest tensile stress found at a given point in a stress field, or the smallest compressive stress if no tensile stresses exist, and is used in the prediction of failure of brittle materials.

Once the Weibull parameter and characteristic strength of a material are known, the probability of failure of a sample of the material subjected to a specified set of loads can be determined. This is done by simply evaluating Equations 1 and 2 to find a value for F. This is then the probability that a given sample will fail because it contains a critical flaw likely to cause the sample to break when the specified loads are applied. For example, if a value of 0.01 is found for F, then one out of every hundred samples constructed of the material and subjected to the specified loads is likely to break.

Traditionally, evaluation of the parameters necessary to describe such a probability of failure has required strength testing of professionally prepared samples having uniform, easily described geometries. These samples may be in the form of small beams for three or four point bend tests, circular or C-shaped rings to be tested in tension or compression, or specially designed cylindrical tension specimens [9]. What these samples all have in common is their strict dimensional uniformity and surface preparation requirements. When such samples are used, the data can be fit to Equation 1 in a straight forward manner to determine the values of m and σ_o which are representative of the material.

However, use of these ideal samples is not always possible. For example, the cost of preparing or obtaining such samples may be prohibitive, the process of producing such samples may alter or destroy a flaw distribution whose effects are to be studied, the dimensions of available stock material may be unsuitable for production of such samples, or sufficient time may not be available to produce such high quality samples. To systematically deal with this problem, a new analysis technique was developed in the present study to allow calculation of the Weibull parameter and characteristic strength of a material, using the results of fast fracture testing of samples of variable geometry.

3.2 Equivalent Load Method

The new technique developed, called the equivalent load method, is centered around the computation of an equivalent load which, if applied to some standardized geometry, would result in the same probability of failure as the actual specimen when it was subjected to the true applied load. This standard geometry may represent an ideal form of the actual samples being tested or may be entirely different.

The theoretical basis for this technique is based on an extension of Jadaan's work with strength of ceramics [12].

Jadaan presented Equations 1 and 2 along with a method for equating the probability of failure of two specimens with different geometries or loading configurations once the Weibull parameter (m) is known. That relationship reduces to a statement that if two samples are made of the same material and have equal probabilities of failure, the integral of σ^m over the surface area of each of the samples will be the same. That is, the probability of failure F is the same for two samples when

$$\int \sigma_a^m dA_a = \int \sigma_s^m dA_s. \tag{3}$$

If the stress distribution in a sample (σ), expressed in MPa, is proportional to a single load value, then it can be written as $P \cdot \sigma_u$ where P is the magnitude of the load, expressed in Newtons, applied to produce the actual stress distribution and σ_u is a stress distribution produced per unit load, expressed in MPa/N. So,

$$\sigma_u = \frac{\sigma(P)}{P} \tag{4}$$

where $\sigma(P)$ is the distribution of maximum principal normal stresses produced by load P. This substitution should be valid for any linear elastic material subjected to small deflections. Most ceramic materials, including the material evaluated in this study, will satisfy these requirements. Written in this form, two samples with different geometries will have equal probabilities of failure if the following generalization of Jaadan's theory holds true.

$$P_s^m \int \sigma_{u_s}^m dA_s = P_a^m \int \sigma_{u_a}^m dA_a \tag{5}$$

This can then be rearranged into the following form.

$$P_s = P_a \left(\frac{\int \sigma_{u_a}^m dA_a}{\int \sigma_{u_s}^m dA_s} \right)^{\frac{1}{m}} \tag{6}$$

This equation then provides a way to compute an equivalent load P_s which, if applied to some standardized geometry with surface area A_s, would result in the same probability of failure as the actual specimen with surface area A_a had when the true load P_a was applied. However, this expression is a function of m which is initially unknown. Therefore, in practice, an iterative solution technique must be used whereby a value of m is guessed, the equivalent loads for each of the specimens are computed using Equation 6, and the resulting data is fit to Equation 1 using traditional techniques. If the value of m found by fitting the data to Equation 1 is different than the value used to compute the equivalent loads using Equation 6, this is not the true value of m which best matches the experimental data collected. Therefore, the process must be repeated using a different value of m in Equation 6 and again fitting the resulting data to Equation 1. Eventually a value of m will be found which will satisfy both equations. Once this is known, the characteristic strength σ_o can also be computed.

3.3 Maximum Likelihood Criteria

Traditional methods of fitting data to Equation 1 usually involve either a least squares or maximum likelihood criteria. Since the maximum likelihood method requires an iterative solution, it may easily be combined with the equivalent load method described above. A single iteration series can be used which will find a value of m which will satisfy all of the necessary requirements.

The log likelihood function (l) associated with the distribution function (F) given in Equation 1 and applied to a set of n experimental samples can be written as

$$l = nLog(m) - m \cdot nLog(\sigma_o) - \frac{1}{\sigma_o^m}\sum_{i=1}^{n}\left(\int \sigma_i^m dA\right) + \sum_{i=1}^{n}\left(Log\int \sigma_i^{m-1} dA\right) \quad (7)$$

where n is the number of samples to be analyzed, and σ_i is the stress distribution in the ith specimen. The values of m and σ_o which maximize the value of l are the values which allow the best fit or description of the data set under consideration. To find these values, the partial derivatives of l with respect to each of the unknown parameters can be set equal to zero. A solution to the resulting equations results in either a maximum or minimum value of l. In this case, the maximum point is always located, because for poor values of m and σ_o the likelihood function decreases without bound and has no minimum point.

Setting the derivative of l with respect to σ_o equal to 0, and solving for σ_o gives

$$\sigma_o = \left(\frac{1}{n}\sum_{i=1}^{n}\int \sigma_i^m dA\right)^{1/m} \quad (8)$$

By substituting this expression for σ_o back into Equation 7 before solving for m, the value of σ_o need not be computed until after m is found. After such a substitution, setting the derivative of l with respect to m equal to 0 gives

$$m = n\left(n\frac{\sum_{i=1}^{n}\int \sigma_i^m Log(\sigma_i)\, dA}{\sum_{i=1}^{n}\int \sigma_i^m\, dA} - \sum_{i=1}^{n}\left(\frac{\int \sigma_i^{m-1} Log(\sigma_i)\, dA}{\int \sigma_i^{m-1}\, dA}\right)\right)^{-1} \quad (9)$$

Applying the assumption that the stress distribution σ can be written as $P \cdot \sigma_u$, and that the same σ_u can be used for all of the samples allows Equation 9 to be

rewritten as

$$m = \frac{n}{Integrals + Sums}$$

where

$$Integrals = n\frac{\int \sigma_u^m Log(\sigma_u)\, dA}{\int \sigma_u^m\, dA} - n\frac{\int \sigma_u^{m-1} Log(\sigma_u)\, dA}{\int \sigma_u^{m-1}\, dA} \qquad (10)$$

and

$$Sums = n\frac{\sum_{i=1}^{n} P_i^m Log(P_i)}{\sum_{i=1}^{n} P_i^m} - \sum_{i=1}^{n} Log(P_i)$$

while the expression for σ_o found in Equation 8 becomes

$$\sigma_o = \left(\frac{\sum_{i=1}^{n} P_i^m}{n} \int \sigma_u^m dA\right)^{1/m} \qquad (11)$$

A more complete derivation of these expressions can be found in Appendix A.

3.4 Summary of Solution Sequence

Equations 6, 10, and 11 are then all that is needed to implement the following solution procedure.

(1) Choose a standard geometry to be used for computation of equivalent loads.

(2) Determine the stress distribution (σ_{u_s}) in the standard geometry when a unit load ($P_s = 1$ N) is applied.

(3) Determine the stress distribution (σ_{u_i}) in each of the actual samples.

(4) Choose a "First Guess" value for m.

(5) Use Equation 6 to determine the equivalent load for each of the specimens.

(6) Use Equation 10 to compute m.

Note: the $\sum_{i=1}^{n} Log(P_i)$ term need only be computed once for each sample set, but the other two sums and the four integrals must be recomputed at each iteration because they are dependent on the value of m.

(7) If the m computed in step (6) is the same as the m used in step (5) then use Equation 11 to find σ_o and the solution is complete. If the two values of m do not match, choose a new m somewhere between the value used in step (5) and the one computed in step (6) and return to step (5). A value half way between the two will often work, though in some cases a value closer to that used in step (5) resulted in faster convergence in the present study.

3.5 Restrictions to the Equivalent Load Method

While the new method of analysis allows the use of samples which would not be suitable for analysis using traditional methods, some restrictions must still be imposed. The first of these restrictions is that the critical flaws in each of the samples must be members of the same flaw population. This condition will usually be satisfied if all of the samples come from the same stock material and have been prepared and or treated in a similar fashion. The second restriction is that the stress distribution within each sample at the time of fracture must be known. If the geometry and loading of each sample can be accurately described, such a stress distribution can usually be determined. If an exact solution is not available due to irregular geometry or complex loading, a numerical method such as finite element analysis can often be used to find a reasonable approximation of the stress distribution.

It is this second restriction that may be the limiting factor in the accuracy of these calculations. While the load applied to a sample at the time of fracture is usually known, an accurate description of the geometry may be more difficult to obtain. For the ideal specimens used in traditional analysis, the geometry can usually be fully described by a small number of dimensions. However, if the geometry is irregular, a larger number of well placed measurements will be

needed. Furthermore, because of the larger number of dimensions which must be determined, it may not be practical to make repeated measurements of each dimension to reduce measurement error. The effects of measurement error may be reduced by applying some sort of "smoothing" to the dimensions. This can be done by fitting a continuous function to the measured data points. In addition to reducing the effects of measurement error, this will convert the coarse discrete data available from the measurements into a continuous description of the geometry which can then be more easily modeled for computation of the stress distribution.

3.6 Application of the Equivalent Load Method

The problem for which this solution technique was developed involves the compression testing of C-rings of somewhat irregular geometry. There were two sources of irregularity in the geometry of the specimens. First, the wall thickness of the tubes from which the samples were made was irregular. According to the manufacturer, a variation of up to 15% above or below the nominal value of the wall thickness was unavoidable. This was directly related to the techniques used to manufacture the tubes. The second source of irregularity in the present study was that the equipment needed to cut the tubes into rings of uniform width was not available. Use of the equipment that was available resulted in some variation in the width dimension both from one location to another on a given ring, and from one ring to the next.

The standard geometry chosen for computation of equivalent loads was a C-ring of uniform cross-section. The dimensions used were close to the dimensions of the actual samples. Though it was not necessary to use a standard geometry similar to the actual geometry, doing so provided some verification that the process was working correctly. If the values of the equivalent loads were much different

than the actual loads, while the actual geometry and the standard geometry were very close, that would have provided an indication that something was wrong either with the theory developed or the implementation of that theory.

The stress distributions for the standard geometry, as well as each of the actual geometries, was determined using a finite element model. A variety of mesh densities and element types were tried before deciding to use a mesh consisting of 707 2D 9-node isoparametric elements. Appendix B provides a more detailed description of the finite element models used. Since both the actual and standard geometries produced stress distributions which were proportional to a single load value, all of the finite element models were solved for a unit load of one Newton. Assuming that the material failure can be attributed to a surface distribution of material flaws, the desired output of the finite element model consisted of a maximum principal normal stress value and a corresponding surface area for each of the finite elements on the outer surface. Maximum principal normal stresses were used because of the tendency of ceramics to fail due to tensile stresses. If the maximum principal normal stress was negative, indicating a compressive stress, then a value of zero was reported since compressive stresses will not generally contribute to the failure of brittle materials such as ceramics.

While the geometry of the standard C-ring was exactly specified, the actual C-ring geometries involved some approximations. For each of the specimens, 10 measurements were taken. These described the width and thickness of the specimen at each of 5 points equally spaced over the portion of the sample experiencing stress during testing. To convert this data into a continuous description of the geometry, the thickness of the material was fit with a cubic polynomial, while the width was fit with a parabola. For most of the samples, the radius of the outer

surface of the rings was nearly constant. However, for one of the data sets, specifically those obtained at 1400°C With Slag, the outer radius was also non-uniform. For that data set, 9 diameter measurements were taken for each specimen, and were fit with a sine and cosine series.

A number of fit functions were tried before those were selected. The selection of functions to be used for fitting was based on attempts to match visible patterns in the dimensional irregularity found in the experimental data. Additional measurements of a subset of the full sample were taken and used to verify the ability of these functions to provide a reasonable description of the true sample geometries. As discussed earlier, an additional benefit of this sort of smoothing of the data is that it reduces the effects of measurement error. The alternative to using a curve fit of some sort would be to take multiple measurements of each of the desired dimensions, and to measure a large number of dimensions. Then, the multiple measurements could be averaged to reduce measurement error, and the large number of known dimensions would provide a nearly continuous description of the geometry. This would have required more time, or more advanced equipment than was available.

A computer program was written to implement the iterative solution sequence described above. The source code for this program is provided in Appendix C. The integrals found in Equations 6, 10, and 11 were evaluated by summing the appropriate values computed using the outputs of the finite element analysis for each sample. After each loop, the value of m computed from Equation 10 was compared to value of m used to initiate that loop. If these two values were not sufficiently close to each other, a new initial value of m was taken as the average of them and the iteration loop summarized in Section 3.4 was repeated. In a few cases, this resulted in an extremely slow convergence rate. Therefore, if a final

value was not found after 50 iterations, new values of m would then be computed as $\frac{3}{4}$ of the previous value plus $\frac{1}{4}$ of the newly computed value.

Once a final value of m was determined, Equation 11 was used to compute σ_o. In addition to the values of m and σ_o, the equivalent load values and estimated probability of failure for each of the specimens were provided as outputs. The results of this analysis will be presented in Chapter 4.

3.7 Limitations to the Equivalent Load Method

Because this technique was recently developed, it has not been fully tested and may contain limitations which have not yet been discovered. One significant problem has been identified. This arises when the data to be fit is such that it does not closely approach a Weibull distribution. This can occur when the critical flaws are not members of a single population or when data sets from different materials are combined and fitted as a single data set. While no attempt to fit such data to a Weibull distribution will produce good results, one does expect the resulting fit parameters to match the data as closely as is possible. For example, in the case where two different data sets are combined, one would expect the resulting fit parameters to lie between the values associated with the two data sets if evaluated individually. Unfortunately, this is not always what occurs with this analysis method. Therefore, when applying this method, the quality of the the fit must be considered. If a poor fit is produced, further analysis, perhaps based on the assumption of a bimodal failure probability distribution, should be considered.

Chapter 4

Results

4.1 Strength Data

Using the analysis techniques described in Chapter 3, a characteristic strength and a Weibull parameter was determined for each of the tube material sample sets. Table 4.1 gives a summary of the strength data produced from this analysis while Figure 4.1 shows the data from which these results were derived, plotted in the form of the log of minus the log of one minus the probability of failure versus log stress.

Table 4.1

Summary of Strength Results

Exposure Condition	σ_o Characteristic Strength	m Weibull Parameter
Room Temp	410 MPa	10.91
1100°C No Slag	282 MPa	9.06
1100°C With Slag	245 MPa	9.73
1260°C No Slag	226 MPa	12.82
1260°C With Slag	328 MPa	6.80
1400°C No Slag	197 MPa	11.18
1400°C With Slag	149 MPa, 142 MPa	5.86, 13.10

While Table 4.1 gives the necessary values in a form that can easily be applied, it is easier to see the trends in the data by examining Figure 4.1. Each point on

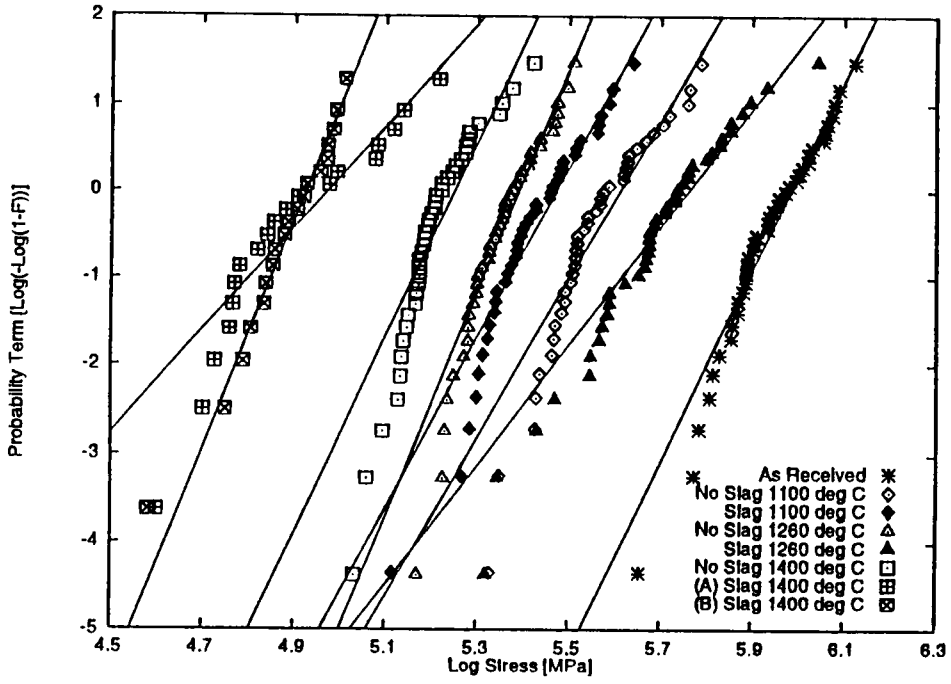


Figure 4.1 Complete Strength Data

this graph represents a test specimen. The horizontal axis represents a log stress value. The stress whose log value is displayed is the stress which would have to be applied to a specimen in uniform tension with a unit surface area of one square millimeter to have the same probability of failure as the given specimen had when the actual load was applied. This value is computed as a numerical approximation of $P(\int \sigma_{u_a}^m dA)^{\frac{1}{m}}$ where P is the actual load applied to a given specimen, σ_{u_a} is the actual stress per unit load for that specimen as computed from the finite element model of the sample, A is the surface area of the specimen, and m is the computed Weibull parameter for the material. So, moving from left to right on the plot represents increasing stress values, and stronger materials.

The vertical axis is related to the probability of failure of a specimen. The actual term plotted is the log of the log of $\frac{1}{1-F}$ where F is the estimated probability of failure of the sample. This means that moving upward on the plot represents an increase in the probability of failure of a sample. The value of the probability of failure F is estimated to be equal to $\frac{i-0.5}{N}$ where N is the number of samples, and i is the rank of the given specimen within the data set when arranged in order of increasing equivalent fracture load. For example, out of a sample of 40, the specimen which failed at the lowest equivalent load is estimated to have a probability of failure of 1.25% since N would equal 40, while i would equal 1. Because a maximum likelihood criteria was used to compute the values of m and σ_o, this estimate was not used during computation, as would have to be done if a least squares fit was used. However, this estimator has been shown to provide a reasonable representation of the probability of failure of such specimens and is generally accepted for graphically displaying test results such as these [10].

When plotted in this way, a data set which fits a Weibull distribution will appear as a straight line. The slope of this line will be the Weibull parameter

m, while the stress value corresponding to the point where the line crosses the 63.2% probability of failure ($\text{Log}(\text{Log}(\frac{1}{1-F})) = 0$) is the characteristic strength σ_o. Each of the data sets produced during this test program appears as a reasonable approximation of a straight line. This confirms that a Weibull analysis can be used satisfactorily to estimate failure probability for these materials.

4.2 Trends and Irregularities in the Analyzed Data

In general, the trends which can be seen in Figure 4.1 match the expected results of a test of this type. Moving from left to right across the plot, from weaker materials to stronger materials, the results of exposing the base material to less harsh conditions are seen. The line of data at the far right represents the virgin material tested at room temperature as it was received from the manufacturer. As expected, the material in this sample set is significantly stronger than any of the other material samples.

At the far left edge of the plot are two lines representing the material exposed to slag at 1400°C. This far left location indicates the weakest of the materials, those material samples which were exposed to this harshest set of the exposure conditions. Note that there is a set of points, and a line which has been fit to it, for samples which were cut from each of the two tubes exposed to this condition. This means that significant differences were experimentally observed in the strength of the material from the two sets of material exposed to the harshest condition.

This was the only condition that resulted in a noticeable loss of material. Because of these macroscopic effects, these two tube samples were most sensitive to variations in the exposure conditions. This type of sensitivity is believed to have resulted in the two different slopes (m values) of these lines. Because these two slopes are so different, a single Weibull distribution could not accurately be fit to

the combined or full data set. As discussed in Section 3.7, attempts to do so may result in significant error in the calculation of the material parameters. Therefore, the results of fitting these data sets independently are shown. The similarity in the horizonal position of these two lines on the plot indicates that average strength of the material from the two tubes was nearly the same. However, the difference in the slope of the two lines indicates that the failure characteristics when subject to the same loads was significantly different. For all of the other test conditions, this type of variation was not seen. Therefore, each of the other exposure conditions is shown as a single line of points, indicating consistent material failure characteristics.

The next line of data points to the right represents samples which were held at 1400°C for 200 hours in a clean furnace before failure testing. This is followed by data from the results of exposure to 1260°C without slag, 1100°C with slag, and 1100°C without slag. From these data sets, a clear pattern of failure strength behavior can be recognized. As expected, a decrease in exposure temperature results in less loss of strength and better resistance to failure, and material which was not exposed to slag is stronger than material exposed to slag at the same temperature.

However, the one set of data does not follow this pattern. The line of points representing the results of testing the material exposed to slag at 1260°C shows an anomalous behavior. It appears stronger than it should be based on exposure condition. Its position seems to indicate that this material is stronger than any of the three previously mentioned materials all, of which were exposed to less harsh environments.

The explanation for these unexpected results is related to the nature of the slag coating on the material test C-rings that was produced at this temperature. As was mentioned in Chapter 2, those tubes which were exposed to slag at 1260°C

developed a thick, hard, glassy, bubble filled slag layer which was firmly bonded to the tube. Before cutting the mechanical test specimens, most of this slag was removed. However, it was not possible to remove all of the slag without damaging the base material. Therefore, after cutting the C-shaped rings, the slag coat was ground down to a nearly uniform layer approximately 1 mm thick. It was expected that, upon reheating the samples in preparation for fracture, the remaining slag would soften and have little effect on the strength testing. However, this does not seem to have happened.

The high apparent strength of the material suggests that the remaining slag layer provided a significant amount of additional strength to the sample during the mechanical testing. Visual inspection of the slag after fracture confirms that, while it may have softened somewhat, it remained in a stable solid state. At the points of load application, some lasting compression of the slag layer is often visible, but not to the extent that would be expected for the softened, fluid-like material that was expected to form at this temperature.

Examination of the fractures themselves provide some additional clues as to the properties of the slag layer and its effects on the measured strength of the overall sample. The first thing that is noticed about many of the fractures is that the slag layer often has well defined fracture surfaces with little evidence of plastic deformation. This provides further evidence that the slag coat maintained a well defined solid structure throughout the test. Secondly, the fracture locations are often found to coincide with the location of thin areas that resulted in the slag coat after most of the slag was removed. These thin areas were often the result of a large bubble in the slag. This suggests that nonuniformities in the slag coat may have introduced stress concentrations which influenced the location of the fracture.

As a result of these observations, the stress values computed based on the assumption of a non-load bearing slag layer must be discarded. Therefore, the line of data points labeled "1260°C With Slag" in Figure 4.1 must be considered as a representation of the effects of a slag layer on the apparent fracture strength of the ceramic material. One method of extracting useful information from this data is to assume that the slag coat can be modeled as a layer of homogeneous linear elastic material firmly bonded to the ceramic ring. While this is probably not entirely accurate, it may allow a reasonable approximation model for such a structure. By making this assumption, a modified finite element model can be created and solved for each of the specimens exposed to this environment. This then would allow a revised Weibull distribution to be computed.

Even if the linear elastic surface layer model assumption is valid, this still leaves one additional problem that did not exist for the previous finite element models. When a single material is used throughout a finite element model, the value used for the modulus of elasticity for that material will not effect the resulting stress values. However, when two different materials are to be used, such as the base ceramic material and the slag material, the stress values will be dependent on the ratio of the moduli of elasticity used for the two materials. Therefore, without some way of measuring or computing the relative modulus of elasticity of the slag material (at the test temperature), no absolute results can be obtained. However, the revised modeling approach can be exercised by doing a parametric study of the effects of the ratio of elastic moduli on Weibull analysis.

Figure 4.2 shows the results of an analysis of the strength results of the specimens exposed to this set of conditions (1260°C, slag) based on a finite element stress determination using a number of elasticity ratios. What this shows is that, the effect of adding a layer of homogeneous linear elastic material to the outside

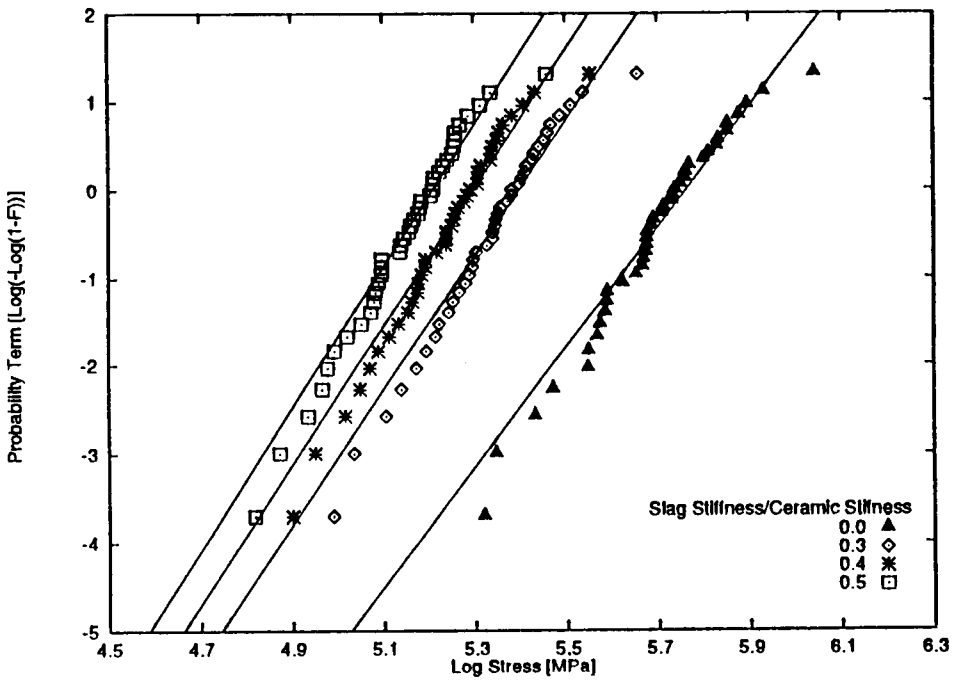


Figure 4.2 Strength Data for the Tube Material Exposed to Slag at 1260°C as a Function of the Ratio of Modulus of Elasticity of the Tube and Slag Material

surface of the test specimens is to adjust the reported characteristic strength of the material while not causing a significant change in the Weibull parameter. This results in the shifting of the line of experimental data from left to right without a noticeable change in the slope of the line. Therefore, while the value of the characteristic strength reported in Table 4.1 for the material exposed to this condition is of little value, the Weibull parameter is believed to be reasonably accurate.

4.3 Rate of Strength Reduction

All of the results presented are based on exposure of the tube samples to the given conditions for a period of 200 hours. Since no variation in the amount of exposure time was used, no conclusive statements can be made about what will happen if these exposure conditions are maintained for longer periods of time. To do so, additional tests are required. However, there are a number of factors which provide clues about what additional testing time may do to the material strength.

The samples exposed to slag at 1400°C showed a significant amount of material loss during this test program. There is no obvious mechanism present which would inhibit removal of additional material. Therefore, it seems reasonable to assume that under these conditions the base material is removed at a constant rate. During these tests a maximum reduction in the tube wall thickness of 1 mm was not uncommon. This suggests that portions of the tube wall would be completely destroyed in as little as 1000 hours of continuous exposure. This would clearly be unsuitable for industrial applications.

For the remainder of the exposure conditions, the lack of visible evidence of corrosion provides little information about the mechanisms responsible for the reduction in strength. This makes estimation of rate information more difficult. However, preliminary theoretical modeling of the reaction mechanisms at work in

this system may provide some insight. This work, being conducted by researchers at the University of Pennsylvania under their subcontract to UTSI, has suggested that the different phases in this composite material may be affected at different rates. Therefore, it is possible that the aluminum alloy phase may be completely destroyed before any significant damage has been done to the SiC and Al_2O_3 ceramic phases. This could cause a slight initial reduction in strength followed by a much longer period of negligible strength change. If this is the case, the strength values found during this test program may be relatively constant for a wide range of time values. Hopefully, additional study of these reaction mechanisms will be able to either refute or support this possibility.

4.4 Modulus of Elasticity for Tube Sample Materials

In addition to the strength and reliability data generated from the Weibull analysis, it was possible to estimate the modulus of elasticity of the material under the different exposure conditions. This was done by comparing the slope of the load deflection curves recorded during testing to the load deflection ratio computed using the finite element model, using an assumed 1MPa unit modulus of Elasticity. These terms are related in the following way.

$$E = \frac{R_e}{R_u} \tag{12}$$

where E is the modulus of elasticity in MPa, R_e is the experimentally determined ratio of load to deflection in Newtons per millimeter, and R_u, expressed in millimeters, is the ratio of load to deflection per unit modulus of elasticity. The results of these calculations based on experimental material behavior, averaged for each of the exposure conditions, are shown in Table 4.2.

Table 4.2

Modulus of Elasticity Results

Temperature	Elastic Modulus After Slag Exposure	Elastic Modulus Without Slag
Room Temp	N/A	276 MPa
1100°C	192 MPa	208 MPa
1260°C	133 MPa	174 MPa
1400°C	95 MPa	133 MPa

As with the strength data, these values follow expected trends. As the temperature is increased, the material becomes more flexible, as indicated by a lower modulus of elasticity. Application of slag simply increases the magnitude of the change. However, the values of elastic modulus computed for the material exposed to slag at 1260°C with slag probably are somewhat in error.

Chapter 5

Conclusions and Recommendation

This study has attempted to determine the strength of $SiC_{(p)}/Al_2O_3$ ceramic matrix composite tube materials produced by Lanxide Corp. after being exposed to both elevated temperatures and elevated temperature with periodically refreshed coal slag, for temperatures up to 1400°C. Unavoidable variations in the as-manufactured geometry of the samples which were used for strength testing, meant that it was not possible to use directly traditional analysis techniques to interpret the strength data obtained. Therefore, new data analysis techniques were developed and used based on the computations of equivalent loads for each of the test specimens.

This new analysis method has shown that the strength of the ceramic composite material continually decreased as the temperature of testing was increased for fixed exposure times. Addition of coal slag to the exposure environment resulted in a further decrease in strength. However, only after exposure to coal slag at 1400°C was a measurable loss of material observed. This suggests that rapid corrosion clearly makes the material unsuitable at and above this temperature level. However, the 30% to 50% reduction in characteristic strength observed at lower temperatures may remain relatively constant over longer periods of time permitting the use of this material at temperatures up to at least 1260°C in heat exchanger tubes and other applications. Values were given in Table 4.1 for the Weibull parameter m and characteristic strength σ_o of the material under the

various test conditions. Using these, along with Equations 1 and 2, it is possible to calculate the probability that a tube made of this material will fail when subjected to a given set of physicals loads under the conditions tested.

However, additional work is needed to increase the usefulness of this data. Continued work is needed to better describe the time-dependent nature of the material strength parameters and also to further refine estimates of the maximum temperature at which this material can survive in this highly corrosive environment. The manufacturer is continuing to make changes to this product, and to the material manufacturing techniques in an attempt to reduce costs and improve dimensional consistency of tubes made with this material. If tighter dimensional tolerances can be met, additional strength testing will be greatly simplified, and designs using the resulting tubes will become much more reliable. As material produced by these new techniques becomes available, additional testing will also be needed to evaluate any resulting changes in strength and high-temperature corrosion resistance of the material.

List of References

List of References

[1] C. SMITH, private communications (February 1995).

[2] "Coal-Fired High Performance Power Generating System – Quarterly Progress Report", DOE/PC/91155-T1 (United Technologies Research Center, East Hartford, CT, 1992) pp. 17-19.

[3] W. H. BOSS and S. BABU, "An Investigation into the Feasibility of a Radiant Recuperative Air Heater for a Magnetohydrodynamic/Steam Power Plant – Topical Report" DOE-ET-10815-139 (United States Department of Energy, 1991) pp. 110-111.

[4] W. H. BOSS, private communication (February 1995).

[5] J. P. WINKLER, MS Thesis, University of Tennessee Space Institute (1992) p. 66.

[6] K. BREDER and V. J. TENNERY, in "Proceedings of the Tenth Annual Coal Preparation, Utilization, and Environmental Control Contractors Conference", Vol. 2 (U.S Department of Energy Pittsburgh Energy Technology Center, Pittsburgh, PA, 1994) pp. 347-357.

[7] K. BREDER, private communication (February 1995).

[8] "Refractory Pocket Catalog", (A. P. Green Industries, Inc. Mexico, Missouri) p. 40.

[9] D. W. RICHERSON, "Modern Ceramic Engineering – Properties, Processing, and Use in Design" (Marcel Dekker, Inc., New York, 1982) pp. 82-89, 318.

[10] J. D. SULLIVAN, P. H. LAUZON, *Journal of Materials Science Letters* 5 (1986) p. 1245.

[11] A. De S. JAYATILAKA, K. TRUSTRUM, *Journal of Materials Science* 12 (1977) pp. 1426-1430

[12] O. M. JADAAN, D. L. SHELLEMAN, J. C. CONWAY, J. J. MECHOLSKY, and R. E. TRESSLER, *Journal of Testing and Evaluation* Vol. 19, No. 3, (May 1991) pp. 181-191.

Appendices

Appendix A
Derivation of Weibull Equations

Given:

$$F = 1 - e^{-KA\left(\frac{\sigma_{max}}{\sigma_o}\right)^m} \tag{A.1}$$

and

$$KA = \int \left(\frac{\sigma}{\sigma_{max}}\right)^m dA \tag{A.2}$$

Substituting the expression for KA from Equation A.2 into the expression for F in Equation A.1 gives

$$F = 1 - e^{-\left(\frac{\sigma_{max}}{\sigma_o}\right)^m \int \left(\frac{\sigma}{\sigma_{max}}\right)^m dA} \tag{A.3}$$

This simplifies to

$$F = 1 - e^{-\frac{1}{\sigma_o^m} \int \sigma^m dA} \tag{A.4}$$

The likelihood function L associated with a function F is defined as

$$L = \prod_{i=1}^{N} \frac{\partial F}{\partial \sigma_i} = \prod_{i=1}^{N} f_i \tag{A.5}$$

where f_i is the partial derivative of F_i with respect to σ_i, and N is the number of specimens. So, with f_i obtained for the failure probability F as

$$f_i = \frac{m}{\sigma_o^m} \left(\int \sigma_i^{m-1} dA_i \right) e^{-\frac{1}{\sigma_o^m} \left(\int \sigma_i^m dA_i \right)} \tag{A.6}$$

then the likelihood function can be written as

$$L = \prod_{i=1}^{N} \frac{m}{\sigma_o^m} \left(\int \sigma_i^{m-1} dA_i \right) e^{-\frac{1}{\sigma_o^m} \left(\int \sigma_i^m dA_i \right)} \tag{A.7}$$

From this, the log likelihood function l is defined as

$$l = \log L = \log \prod_{i=1}^{N} \frac{m}{\sigma_o^m} \left(\int \sigma_i^{m-1} dA_i \right) e^{-\frac{1}{\sigma_o^m} \left(\int \sigma_i^m dA_i \right)} \tag{A.8}$$

Equation A.8 simplifies to

$$l = N\log m - Nm\log\sigma_o + \sum_{i=1}^{N}\log\left(\int \sigma_i^{m-1}dA_i\right) - \frac{1}{\sigma_o^m}\sum_{i=1}^{N}\left(\int \sigma_i^m dA_i\right) \qquad (A.9)$$

The values of σ_o and m which maximize the log likelihood function can be found by setting the derivatives of l with respect to each of these parameters equal to zero, and solving for them. The derivative with respect to σ_o is

$$\frac{\partial l}{\partial \sigma_o} = \frac{-Nm}{\sigma_o} + \frac{m}{\sigma_o^{m+1}}\sum_{i=1}^{N}\left(\int \sigma_i^m dA_i\right) \qquad (A.10)$$

Setting this equal to zero, and solving for σ_o gives

$$\sigma_o = \left(\frac{1}{N}\sum_{i=1}^{N}\left(\int \sigma_i^m dA_i\right)\right)^{\frac{1}{m}} \qquad (A.11)$$

By substituting this expression back into the expression for l before solving for m, it is possible to determine m before determining σ_o. Such a substitution gives

$$l = N\log m + N\log N - N - N\log\left(\sum_{i=1}^{N}\left(\int \sigma_i^m dA_i\right)\right) + \sum_{i=1}^{N}\log\left(\int \sigma_i^{m-1}dA_i\right) \qquad (A.12)$$

Taking the partial derivative of this expression with respect to m gives

$$\frac{\partial l}{\partial m} = \frac{N}{m} - \frac{N\sum_{i=1}^{N}\left(\int \sigma_i^m \log\sigma_i dA_i\right)}{\sum_{i=1}^{N}\left(\int \sigma_i^m dA_i\right)} + \sum_{i=1}^{N}\frac{\int \sigma_i^{m-1}\log\sigma_i dA_i}{\int \sigma_i^{m-1}dA_i} \qquad (A.13)$$

Setting this expression equal to zero gives

$$m = N\left(\frac{N\sum_{i=1}^{N}\left(\int \sigma_i^m \log\sigma_i dA_i\right)}{\sum_{i=1}^{N}\left(\int \sigma_i^m dA_i\right)} - \sum_{i=1}^{N}\frac{\int \sigma_i^{m-1}\log\sigma_i dA_i}{\int \sigma_i^{m-1}dA_i}\right)^{-1} \qquad (A.14)$$

If the stress distribution σ_i can be equated to the product of a load value P_i multiplied by a stress per unit load σ_{u_i}, $\sigma_i = P_i\sigma_{u_i}$, this equation can be rewritten as

$$m = \left(\frac{\sum_{i=1}^{N}\int P_i^m \sigma_{u_i}^m \log P_i\sigma_{u_i} dA_i}{\sum_{i=1}^{N}\left(P_i^m \int \sigma_{u_i}^m dA_i\right)} - \sum_{i=1}^{N}\frac{\int P_i^{m-1}\sigma_{u_i}^{m-1}\log P_i\sigma_{u_i} dA_i}{NP_i^{m-1}\int \sigma_{u_i}^{m-1}dA_i}\right)^{-1} \qquad (A.15)$$

If all of the σ_{u_i} are equal to a single σ_u and all of the A_i are equal to a single A then this can be rewritten as

$$m = \left(\frac{\sum_{i=1}^{N} P_i^m \log P_i}{\sum_{i=1}^{N} P_i^m} + \frac{\int \sigma_{u_i}^m \log \sigma_u dA}{\int \sigma_u^m dA} - \frac{1}{N} \sum_{i=1}^{N} \log P_i - \frac{\int \sigma_u^{m-1} \log \sigma_u dA}{\int \sigma_u^{m-1} dA} \right)^{-1} \tag{A.16}$$

while the expression for σ_o can be rewritten as

$$\sigma_o = \left(\frac{\sum_{i=1}^{N} P_i^m}{N} \int \sigma_u^m dA \right)^{\frac{1}{m}} \tag{A.17}$$

Appendix B
Finite Element Models

The stresses in each of the samples were determined using finite element analysis. A finite element preprocessor and solver were written to perform the necessary calculations. The source code for these programs has not been included due to its size, but is available at UTSI. The code developed to build and analyze these finite element models was in two parts. The first part was a specialized non-interactive preprocessor. The purpose of this code was to create a file containing a detailed description of the finite element mesh needed to describe a given sample along with the applied load and the necessary constraints. A structured mesh consisting of 101 rows of 7 elements each was used. Each of these two dimensional elements was defined by 9 nodes; one node at each of four corners, one node at the middle of each of the four resulting edges, and a final node at the center of the element. The mesh was organized to minimize the amount of deviation of these elements from the ideal square shape which would give the greatest accuracy. The number of elements necessary to produce reasonable results was determined by comparing the computed results obtained with several models of ideal C-shaped rings with, a variety of mesh densities, to theoretical stresses computed from the theory of bending of ideal homogeneous precurved beams of uniform cross section.

The mesh files were then read by a second program which solved the finite element model to determine the stresses. That program was a basic linear finite element solver. The heart of the program consists of routines to build the global stiffness matrix in skyline format and then determine the nodal displacements by solving for the displacement vector using Gauss Elimination by inverting the stiffness matrix. Once the nodal displacements were computed, the strain, and the stress distribution in each of the elements were calculated. These expressions for

the stress distribution in each of the elements, parabolic in each of the two coordinate directions, were then used to compute an average value for the maximum principal normal stress for each of the elements on the outer surface of the sample. Because these are surface elements, this maximum principal normal stress is the stress component tangential to the exposed surface. The remaining components, normal and shear stress on the exposed surface, cannot exist on free surfaces except at the point of application of a physical load. A list of these stress values, along with the surface area over which they appear, was written to an output file providing the input data needed to numerically integrate the maximum principal normal stress, raised to an arbitrary power, over the surface area of the sample. A detailed description of the theory and implementation of these ideas can be found in any elementary text on the finite element method.

Appendix C

Statistical Analysis Code

The following pages contain the source code for the program written to compute σ_o and m for a data set produced by the finite element code described in Appendix B. The code is written in ANSI standard C, and should be usable on a variety of platforms.

```
#include <stdio.h>
#include <stdlib.h>
#include <math.h>
#include <string.h>

struct tension_volume{ /* used to store a stress value and a */
  double t;            /* volume or area value */
  double v;
};

/* data structure:
** constants            ns = number of samples
**                      pps = number of data points per sample
**
** input data values    **tvp points to an array of ns pointers each of which
** (tension,volume)     in turn point to an array of pps tension_volume
**                      structures containing the value of the maximum normal
**                      stress at a point and the volume of that point
**                      within that sample.
**                      *(tvp + i) is a pointer to the start of the data for
**                      the ith sample.
**                      (*(tvp+i)+j)->t is the jth stress value for the ith
**                      sample.
**                      (*(tvp+i)+j)->v is the jth volume value for the ith
**                      sample.
**                              i=1 to ns
**                              j=1 to pps
**                      (*(tvp+i)+0)->v is the actual load value
**                      standardized info is in the ns+1st position
*/

/* readinputs() reads the stress values from a file produced by fea. */
unsigned int readinputs(char infilename[80], /* name of the input file */
                        unsigned int *ns,    /* number of samples read */
                        unsigned int *pps,   /* number of points per sample */
                        struct tension_volume ***tvp_p) /* input data */
{
```

```
  int i,j,error;
  FILE *inputfile;
  struct tension_volume **tvp;

/*  printf("Beginning to read input data\n");*/
/* input file format:  NOTE: all imput values should be due to unit loads
** The first line of the input file contains 2 integers specifying
** the number of samples (ns) and the number of points per samples (pps).
** Then the data for each of the samples is given according to the following
** format.  The data for a given sample will contain *pps+1 lines.  The first
** *pps lines each contain two doubles.  The first is the value of the maximum
** normal stress at that point, and the second is the area over which that
** stress is found.  The *pps+1st line contains a double giving the
** the magnitude of the actual applied load.
**
** after the main data input an additional set of similar data will be given
** for the standard geometry.
*/
  error = 0; /* if error becomes 1, an error has occured */
/* open the input file */
  if((inputfile = fopen(infilename,"r")) == NULL){
    printf("Error opening input file.\n");
    return(0);
  }
/* read the number of samples, and the number of points per sample */
  if ((fscanf(inputfile,"%i %i",ns,pps)) != 2){
    printf("Error reading input header data.\n");
    fclose(inputfile);
    return(0);
  }

/* allocate memory for tvp (pointers to data to be read) */
  if ((tvp = (struct tension_volume * *)
    malloc( (*ns+2)*sizeof(struct tension_volume *) ))==NULL){
    printf("Error allocating memory for input data pointer.\n");
    fclose(inputfile);
    return(0);
  }
  *tvp_p = tvp;


/* allocate memory for arrays of tension_volume data (data to be read) */
  for(i=1;i<=*ns+1;i++){
    if ((*(tvp+i) = (struct tension_volume *)
      malloc( (*pps+1)*sizeof(struct tension_volume) ))==NULL){
      printf("Error allocating memory for input data.\n");
      fclose(inputfile);
      return(0);
    }
  }
```

```
/* begin reading input data */
  for(i=1;i<=*ns+1;i++){
    for(j=1;j<=*pps;j++){
/* the ->t part of the structure holds the stress value,
** while the ->v part of the structure holds the area (or volume)
** assocated with that stress.
*/
      if ((fscanf(inputfile,"%lg %lg",&((*(tvp+i)+j)->t),&((*(tvp+i)+j)->v)))
      != 2) error = 1;
    }
/* read the true load value, stored as the *pps+1st area term */
    if ((fscanf(inputfile,"%lg",&((*(tvp+i)+0)->v))) != 1) error = 1;
  }
/* report of an error has occured while reading the input data */
  if (error == 1){
    printf("Error reading input data.\n");
    fclose(inputfile);
    return(0);
  }
  fclose(inputfile);
  return(1);
} /* end readinputs() */

/* ik returns the value of the intergral of pow(stress,m)
** over the surface (or volume) of the ith sample.
*/
double ik(int i, /* number of sample to be used */
          double m, /* value of m (weibull parameter) */
          struct tension_volume **tvp, /* input data */
          int pps) /* number of points per sample */
{
  int j;
  double returnval,kvalue;
  returnval = 0.0;
  for(j=1;j<=pps;j++)
  {
    kvalue = (*(tvp+i)+j)->t;
    if (kvalue != 0)
      returnval += pow(kvalue,m)*(*(tvp+i)+j)->v;
  }
  return(returnval);
} /* end ik() */

/* iklk returns the value of the intergral of pow(stress,m)log(stress)
** over the surface (or volume) of the ith sample.
*/
double iklk(int i, /* number of sample to be used */
            double m, /* value of m (weibull parameter) */
            struct tension_volume **tvp, /* input data */
            int pps) /* number of points per sample */
{
```

```
  int j;
  double returnval,kvalue;
  returnval = 0.0;
  for(j=1;j<=pps;j++)
  {
    kvalue = (*(tvp+i)+j)->t;
    if (kvalue != 0)
      returnval += pow(kvalue,m)*log(kvalue)*(*(tvp+i)+j)->v;
  }
  return(returnval);
} /* end iklk() */

/* compute KV or KA as defined by Jadaan */
double ikv(int i, /* number of sample to be used */
           double m, /* value of m (weibull parameter) */
           struct tension_volume **tvp, /* input data */
           int pps) /* number of points per sample */
{
  int j;
  double returnval,kvalue,kmax;
  returnval = 0.0;
  kmax = 0.0;
  for(j=1;j<=pps;j++)
  {
    kvalue = (*(tvp+i)+j)->t;
    if (kvalue > kmax) kmax = kvalue;
    if (kvalue != 0)
      returnval += pow(kvalue,m)*(*(tvp+i)+j)->v;
  }
  returnval /= pow(kmax,m);
  return(returnval);
} /* end ikv() */



void writeresults(FILE *outfile, /* file to write to */
                  double m, /* computed value of m (weibull parameter) */
                  struct tension_volume **tvp, /* input data */
                  unsigned int ns, /* number of samples */
                  unsigned int pps, /* number of points per sample */
                  double sig0) /* computed value of sigma_o  */
{
  int     i,j,k;
  double iknm,ikim;
  double *p;
  int *ip; /* ordered list of sample numbers according to load */
  printf("writing outputs to file\n");

/* allocate space for storage of load values */
  p = (double *) malloc((ns+1)*sizeof(double));
  ip = (int *) malloc((ns+1)*sizeof(int));
```

```
/* these values are intended to be human-readable.
** later values will be organized for easy plotting using gnuplot.
** Therefore, lines which are not to be used for plotting are
** preceeded by a # which is the comment symbol in a
** gnuplot data file.
*/
  fprintf(outfile,"# Loads & stress integrals (ikim) & (ikim/iknm)^(1/m)\n");
  iknm = ik(ns+1,m,tvp,pps);
  fprintf(outfile,"# iknm = %lg\n",iknm);
  for(i=1;i<=ns;i++){
    *(p+i) = (*(tvp+i)+0)->v;
    ikim = ik(i,m,tvp,pps);
    *(p+i) *= pow(ikim/iknm,1.0/m);

    fprintf(outfile,"# %i %lg %lg %lg\n",i,*(p+i),ikim,pow(ikim/iknm,1.0/m));
  }
  fprintf(outfile,"# %lg\n",iknm);

  for(k=1;k<=ns;k++)  *(ip+k) = 0;

/* sort samples according to equivalent load */
  for(i=1;i<=ns;i++){
    k=1;
    for(j=1;j<=ns;j++){
      if (*(p+i) > *(p+j)) k++;
    }
    while(*(ip+k) != 0) k++; /* take care of repeated loads */
    *(ip+k) = i; /* put sample number in kth position of ip */
  }

/* write output values (for plotting )*/
  for(k=1;k<=ns;k++)
  {
    i = *(ip+k);
    fprintf(outfile,"%i %g %g ",i,
    log(*(p+i)*pow(iknm,1.0/m)),log(-log(1.0-(k-0.5)/(1.0*ns))));
    fprintf(outfile,"%g %g\n",(k-0.5)/(1.0*ns),
      1-exp(-iknm*pow(*(p+i)/sig0,m)));
  }
  free(p); /* deallocate memory */
  free(ip);
} /* end writeresults() */

/* compute the sums and integrals needed to calculate m (weibull par
void sums(double m,
          struct tension_volume **tvp, /* input data */
          unsigned int ns,             /* number of samples */
          unsigned int pps,            /* number of points pe
          double *allints,             /* return value of t
          double *allsums,             /* return value of
```

```
          double *signot,              /* the value of sigma_o */
          double *l)                   /* the value of l (log liklihood) */
{
  int     i;
  double iknm,iknmmo,iklknm,iklknmmo,ikim,p;
  double sum1, sum2, sum3;
/* compute the value of the terms wich use only the standard geometry */
  iknm = ik(ns+1,m,tvp,pps); /* the integral of pow(stress,m) */
  iknmmo = ik(ns+1,m-1.0,tvp,pps); /* integral of pow(stress,m-1) */
  iklknm = iklk(ns+1,m,tvp,pps); /* integral of pow(stress,m)*log(stress) */
  iklknmmo = iklk(ns+1,m-1.0,tvp,pps);
                               /* integral of pow(stress,m-1)*log(stress) */
  *allints = ns*iklknm/iknm-ns*iklknmmo/iknmmo;
                               /* combination of the above terms */

/* initialize the sums to be computed */
  sum1=0;
  sum2=0;
  sum3=0;
/* sum over all of the samples */
  for(i=1;i<=ns;i++){
    p = (*(tvp+i)+0)->v; /* the true value of the applied load */
    ikim = ik(i,m,tvp,pps); /* integral of ith pow(stress,m) */
    p *= pow(ikim/iknm,1.0/m); /* compute equivalent load */
    sum1 += pow(p,m)*log(p); /* increment sums */
    sum2 += pow(p,m);
    sum3 += log(p);
  }
  *allsums = ns*sum1/sum2 - sum3; /* combine sum terms */
  *signot = pow(sum2/ns*iknm,1.0/m); /* compute sigma_o and l */
  *l = ns*(-1+log(1.0*ns)+log(m)-log(sum2)-log(iknm)+log(iknmmo))+(m-1.0)*sum3;
} /* end sums() */

int main(int argc, char *argv[16]){
/* outline:
**                  read the values from the finite element processor
**                  guess a value for m
**          loop:   compute the integral sums for that m
**                  solve for the m (which maximizes l)
**                  compute lnl (as a check)
**                  if m has changed, goto loop
**                  else compute sig0
**                  end
*/
/* command line options:
**    -i'Input file name'
**    -o'Output file name'
*/
  struct tension_volume **tvp = NULL;
  unsigned int ns,pps,i;
  double oldm,tempm,m,L,sig0;
```

```
  double allints, allsums;
  char infilename[80], outfilename[80];
  FILE *outfile;

  infilename[0] = NULL;
  outfilename[0] = NULL;


/* parse command line options */
  for(i=1;i<argc;i++){
    if (argv[i][0]=='-') {
      if (argv[i][1]=='i') {  /* input file name given */
        strcpy(infilename,&(argv[i][2]));
      }
      if (argv[i][1]=='o') {
        strcpy(outfilename,&(argv[i][2]));
      }
    }
    else{
      printf("\n Invalid command line argument!\n");
      return(1);
    }
  }

  if(infilename[0] == NULL)
    strcpy(infilename,"weibull.in");
  if(outfilename[0] == NULL)
    strcpy(outfilename,"weibull.out");

  if((outfile = fopen(outfilename,"w")) == NULL){
    printf("Error opening output file.\n");
    return(1);
  }

/* read the input data */
/* readinputs() will return a 0 if an error occurs */
  if (readinputs(infilename,&ns,&pps,&tvp)==0) return(1);

  oldm = 10.0;
  m = 1.0; /* the "First Guess" value for m (weibull parameter) */
  i = 0;   /* use i to keep track of the number of itterations */
/* begin main loop.
** solution is considered found when then amount of change between the
** previous m and the new m is less than 1.0e-6 (adjust this value as desired).
*/
  while(fabs(m-oldm) >= 1.0e-6){
    i++;
/* compute the sums and integrals needed to compute the value of m */
    sums(m,tvp,ns,pps,&allints,&allsums,&sig0,&L);
    oldm = m; /* store previous value of m */
    tempm = ns/(allints + allsums); /* compute new value of m */
```

```
    m = (tempm + oldm)/2.0; /* use m half way between new and old */
    if(i>50) m = (m+oldm)/2.0;  /* if oscillating, try to dampen */
    if(m>100.0) m = 100.0;      /* limit m to avoid overflows */
  }

/* write equivalent loads and actual effective volumes to a file */
  writeresults(outfile,m,tvp,ns,pps,sig0);
/* print basic results to file and stdout */
  fprintf(outfile,"# *** m = %g, sig0 = %g, L = %g ***\n",m,sig0,L);
  fclose(outfile);
  printf("m = %lg (sig = %lg) (l = %lg) \n",m,sig0,L);
  printf("kv = %lg iknm = %lg intercept = %lg\n",
  ikv(ns+1,m,tvp,pps),ik(ns+1,m,tvp,pps),-m*log(sig0));

  return(0);
} /* end main() */
```

Vita

Peter Ford LaRue was born in Grand Rapids, Michigan on September 3, 1971. He received his primary and secondary education through the Forest Hills School District in Grand Rapids, MI. He graduated from Forest Hills Northern High School in 1989. He then attended Michigan Technological University in Houghton. Four years later, in May of 1993, he received his Bachelor of Science degree in Mechanical Engineering Then, in May of 1995 he received his Master of Science in Mechanical Engineering from the University of Tennessee.